

Lattice Boltzmann model for predicting the deposition of inertial particles in turbulent channel flows

Guillaume Lepoutère¹, Pascal Fede¹, Victor Sofonea², Richard Fournier³, Stéphane Blanco³, Olivier Simonin¹

¹Institut de Mécanique des Fluides de Toulouse (IMFT) - Université de Toulouse, CNRS, INPT, UPS, FR-31400 Toulouse, France

²Center for Fundamental and Advanced Technical Research, Romanian Academy, RO-300223 Timisoara, Romania

³Laboratoire Plasma et Conversion d'Energie (LAPLACE) - Université de Toulouse, CNRS, INPT, UPS, FR-31062 Toulouse, France

Abstract

The purpose of the paper is the using of a Lattice Boltzmann Model (LBM) for solving the kinetic equation describing the interaction of solid inertial particles with a turbulent flows. The method has been successfully used for particles transported by a homogeneous isotropic turbulent flow field. In the present paper the LBM is used for the prediction of the particle deposition in vertical channel. In such a configuration, according to the Stokes number, the particle agitation may vary strongly with respect to the wall distance through the boundary layer that can be a problem for the LBM. However, the comparison of experimental data with the LBM results show that the deposition rate of particle is well predicted for large Stokes number (inertia dominated regime) and also for moderate Stokes number (impaction-diffusion regime).

Keywords: LBM, gas-particle interaction, deposition, kinetic equation

1. Introduction

Solid inertial particles suspended in turbulent flows are found in many practical applications as sediment transport or ripple motion, coal combustion, particulate radioactive contamination, pollutant deposition, drug inhalation by medicine aerosols.

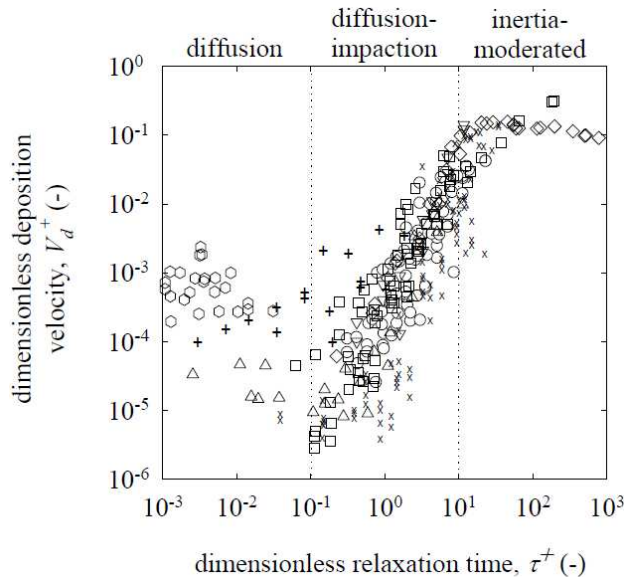


Figure 1: Particle deposition measured in several experiments and gathered by Sippola & Nazaroff [20].

As shown by Figure 1, the particle deposition in turbulent channel flow can be split in three regimes [7]:

- $\tau_p^* \ll 1$: the diffusion regime where the particles behave like tracers and the deposition rate is controlled by the Brownian motion.
- $\tau_p^* \gg 40$: the inertial regime, also called ballistic regime,

where the particles do not interact with the turbulence, and achieve a free flight-like march down to the wall,

- $1 < \tau_p^* < 40$: the intermediate regime, also called diffusion-impaction regime, corresponding to a partial interaction of the particles with the turbulence.

where $\tau_p^* = \tau_p u^{*2} / \nu_f$ is the Stokes number with ν_f / u^{*2} the characteristic wall-turbulence time scale defined on the basis of a wall friction velocity u^* . Finally τ_p is the particle relaxation time

$$\tau_p = \frac{\rho_p d_p^2}{18 \rho_f \nu_f} \quad (1)$$

In parallel to experiments, Direct Numerical Simulation (DNS) or Large Eddy Simulation (LES) coupled with Discrete Particle Simulation (DPS) have been carried out for understanding the local mechanisms involved in particle deposition [12, 24, 11]. These numerical simulations have supported the development of modelling approaches for predicting the deposition rate of solid particles transported by a turbulent flow [21, 2, 25, 17].

In 2009, Aguinaga et al. [1] have proposed an original approach for modelling the dynamic behaviour of solid particles interacting with a turbulent flow. The approach, briefly described in the following section, is based on a statistical description of the particle motion by using a Probability Density Function (PDF). The originality of the approach lie in the closure of the gas-particle interaction term. Indeed that term is separated in two contributions: one for the mean gas-particle interaction and another one for the fluctuating gas-particle interaction. By making an analogy with the BGK model for rarefied gases, the fluctuating contribution is written as an return-to-equilibrium term. Under these closed form, the PDF transport equation can be solve and Aguinaga et al. [1] have shown that this can numerically unstable when the particle Stokes number becomes small. Diounou et al. [5] and later Fede et al. [6] have proposed to use a Lattice Boltzmann Model (LBM). They showed that LBM is able to predict the correct particle deposition in case where the turbulent flow is homogeneous and isotropic.

In the present study the same modelling approach and the same Lattice Boltzmann Model is used but in the case of a ver-

tical turbulent channel flow. In such a configuration, the turbulent properties (fluid agitation and dissipation) vary strongly from the top to the bottom of the turbulent boundary layer. Then the gas-particle interaction vary as well and the ability of the LBM approach may be questionable because the LBM have been developed for equilibrium flows. These issues are discussed in the present paper.

2. Modelling approach

The modelling approach is based on a statistical description of the particulate phase transported by a turbulent fluid flow. The dispersed phase is described by the particle Probability Density Function $f_p(\mathbf{x}, t; \mathbf{c}_p)$ defined such that $f_p(\mathbf{x}, t; \mathbf{c}_p)d\mathbf{c}_p d\mathbf{x}$ is the mean probable number of particles at the time t with a centre of mass located in the volume $[\mathbf{x}, \mathbf{x} + d\mathbf{x}]$, with a translation velocity \mathbf{u}_p in $[\mathbf{c}_p, \mathbf{c}_p + d\mathbf{c}_p]$. From the PDF the mean density number of particles writes

$$n_p = \int f_p d\mathbf{c}_p, \quad (2)$$

the mean particle velocity,

$$U_{p,i} = \frac{1}{n_p} \int c_{p,i} f_p d\mathbf{c}_p, \quad (3)$$

and the particle kinetic stress,

$$\langle u'_{p,i} u'_{p,j} \rangle = \frac{1}{n_p} \int [c_{p,i} - U_{p,i}] \times [c_{p,j} - U_{p,j}] f_p d\mathbf{c}_p. \quad (4)$$

The single particle velocity PDF obeys to the following Boltzmann-like kinetic equation:

$$\frac{\partial f_p}{\partial t} + \frac{\partial}{\partial x_i} [c_{p,i} f_p] + \frac{\partial}{\partial c_{p,i}} \left[\left\langle \frac{du_{p,i}}{dt} \middle| \mathbf{c}_p \right\rangle f_p \right] = \left(\frac{\partial f_p}{\partial t} \right)_{col} \quad (5)$$

where $\langle \cdot | \mathbf{c}_p \rangle$ is the ensemble average conditioned by the particle velocity and i is a summation index. In Eq. (5), the third term on the left-hand-side represents the forces acting on the particles, including the turbulent particle-fluid coupling, and the term on the right-hand-side is the modification of the PDF by the inter-particle collisions. In the present study the particulate phase is very dilute such that this term can be safely neglected. Assuming a large particle-to-fluid density ratio, the forces acting on the particles are reduced to the gravity and the drag. In such a framework, the particle acceleration reads

$$\frac{d\mathbf{u}_p}{dt} = -\frac{\mathbf{u}_p - \mathbf{u}_{f@p}}{\tau_p} + \mathbf{g} \quad (6)$$

where $\mathbf{u}_{f@p}$ is the fluid velocity at the particle position, \mathbf{g} the gravity and τ_p the particle relaxation time.

In the following the PDF transport equation is simplified to the case of a particle-turbulence interaction in a wall boundary layer flow then it can be assumed that $\partial/\partial y \approx \partial/\partial z \approx 0$. Also as τ_p has a given value independent of the instantaneous particle velocity, the kinetic equation governing the wall-normal particle velocity PDF is obtained by integration of Eq. (5) on the velocity components in y - and z -directions. Using Eq. (6) in the third term of Eq. (5) and neglecting gravity, the Boltzmann equation becomes

$$\frac{\partial f_p}{\partial t} + \frac{\partial}{\partial x} [c_p f_p] + \frac{\partial}{\partial c_p} \left[-\frac{1}{\tau_p} (c_p - \langle u_{f@p} | c_p \rangle) f_p \right] = 0 \quad (7)$$

where c_p is the particle velocity component expectation in the x -direction normal to the wall.

The literature dedicated to the modelling of the particle-turbulence coupling in the kinetic equation is abundant [4, 26, 15, 16, 18]. As explained in introduction, the closure is done by the approach proposed by Aguinaga et al. (2009) [1] where the fluid-particle interaction term is split in two contributions: first, the fluid-particle interaction through the mean gas and particle velocities; second, the coupling of the particle fluctuating motion with the fluid turbulence. The last contribution is modelled as a return-to-equilibrium term in a similar manner to the effect the inter-particle interactions in the BGK model [3]. The return-to-equilibrium term requires an equilibrium PDF, f^* , and a given time-scale, τ^* . As shown by Aguinaga et al. (2009) [1], for being consistent with the standard moment equation the time-scale, τ^* , is the particle response time τ_p . The fluid-particle interaction is then written as

$$\frac{\partial}{\partial c_p} \left[-\frac{1}{\tau_p} (c_p - \langle u_{f@p} | c_p \rangle) f_p \right] = - \left[\frac{U_p - U_{f@p}}{\tau_p} \right] \frac{\partial f_p}{\partial c_p} + 2 \frac{f_p - f^*}{\tau_p}. \quad (8)$$

The equilibrium PDF, f^* , is chosen in order to model particles in equilibrium with the gas turbulence according to the Tchen & Hinze theory [22, 8]:

$$\langle u'_p u'_p \rangle = \langle u'_{f@p} u'_{f@p} \rangle = \langle u'_{f@p} u'_{f@p} \rangle \frac{1}{1 + St} \quad (9)$$

with the Stokes number $St = \tau_p / \tau_{f@p}^t$ where $\tau_{f@p}^t$ is the fluid Lagrangian integral time scale seen by the particles. As shown later, the modelling of the such a timescale in turbulent boundary layer is crucial for the particle dispersion. The equilibrium PDF is modelled by a Gaussian distribution [9]

$$f^*(x, t; c_p) = \frac{n_p}{(2\pi \langle u'_{f@p} u'_{f@p} \rangle)^{1/2}} \exp \left[-\frac{(c_p - U_p)^2}{2 \langle u'_{f@p} u'_{f@p} \rangle} \right]. \quad (10)$$

The mean fluid velocity seen by the particles, $U_{f@p}$, has two contributions: i) the mean fluid velocity U_f and ii) a drift velocity U_{drift} representing the correlation between the local instantaneous particle distribution and the turbulent fluid velocity. Then the mean fluid velocity seen by the particles is written as $U_{f@p} = U_f + U_{drift}$ and, following Simonin et al. [19], the drift velocity in homogeneous turbulence reads,

$$U_{drift} = -\tau_{f@p}^t \langle u'_{f@p} u'_p \rangle \frac{1}{n_p} \frac{\partial n_p}{\partial x}. \quad (11)$$

Finally the Boltzmann-like transport equation (7) with the SAB model for the fluid-particle interaction writes

$$\frac{\partial f_p}{\partial t} + c_p \frac{\partial f_p}{\partial x} - \left[\frac{U_p - (U_f + U_{drift})}{\tau_p} \right] \frac{\partial f_p}{\partial c_p} + \frac{2}{\tau_p} [f_p - f^*] = 0. \quad (12)$$

3. Lattice Boltzmann Model (LBM)

The Lattice Boltzmann model used to solve the Eq. (12) is described by Fede et al. [6]. Basically, an approximate form of Eq. (12) is used in which the distribution function f_p appearing in the force term is replaced by a Hermite polynomial expansion of kernel f_p^0 , where

$$f_p^0 = \frac{n_p}{\sqrt{2\pi \langle u'_p u'_p \rangle}} \exp \left[-\frac{(c_p - U_p)^2}{2 \langle u'_p u'_p \rangle} \right] \quad (13)$$

is the local equilibrium distribution function. Then Boltzmann equation projected onto Hermite polynomial basis reads

$$\frac{\partial f_p}{\partial t} + c_p \frac{\partial f_p}{\partial x} - \left[\frac{U_p - (U_f + U_{drift})}{\tau_p} \right] \frac{\partial}{\partial c_p} (Q_{N_h} f_p^0) + \frac{2}{\tau_p} [f_p - f^*] = 0 \quad (14)$$

where Q_{N_h} is a polynomial function of c_p of order N_h (the Hermite expansion order) that depends on all moments of the distribution function of order lower or equal to N_h and f^* is now the its projection onto the Hermite polynomial basis. Then procedure allows to replace the partial derivative $\partial f_p / \partial c_p$ by an explicit function of the moments, transforming the question of choosing a set of discrete velocities into a quadrature choice.

The second step is the quadrature choice itself. Equation 14 involves the following integral quantities appearing in f_p^0 and f^* , and all the moments of the vector appearing in Q_{N_h} . This means that the question is only the evaluation of velocity moments of increasing orders. Here, a Gauss-Hermite quadrature of order N_q is used. Altogether, N_q values $f_{p,\alpha}$ of the distribution function ($\alpha = 1, 2, \dots, N_q$), at discrete velocities $\check{c}_{p,\alpha}$, are considered in their coupled temporal evolutions according to

$$\begin{aligned} \frac{\partial f_{p,\alpha}}{\partial t} + \check{c}_{p,\alpha} \frac{\partial f_{p,\alpha}}{\partial x} - \left[\frac{U_p - (U_f + U_{drift})}{\tau_p} \right] \left[\frac{\partial}{\partial c_p} (Q_{N_h} f_p^0) \right]_{c_p = \check{c}_{p,\alpha}} + \frac{2}{\tau_p} [f_{p,\alpha} - f_{\alpha}^*] = 0 \end{aligned} \quad (15)$$

where U_p , Q_{N_h} and f_{α}^* are the approximations of the corresponding terms in Eq. (14) in which all the moments M_m are replaced by their evaluation as $\sum_{\alpha=1}^{N_q} \omega_{\alpha} f_{p,\alpha} \check{c}_{p,\alpha}^m$ where $\omega_1, \omega_2, \dots, \omega_{N_q}$ are the N_q quadrature weights. α is a free index.

4. Numerical simulation overview

The configuration is an established vertical turbulent channel flow obtained thanks to the DNS of Moser et al. [13]. The deposition rate will be compared to the one obtained by Liu & Agarwal [10].

4.1. Geometry, mesh and boundary conditions

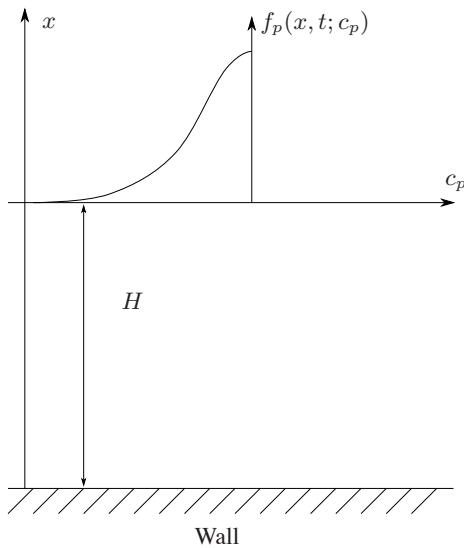


Figure 2: Computational domain.

As explained previously, the problem is one-dimensional in space and one-dimensional in velocity (wall-normal component). The size of the computational domain, shown by Figure 2, is denoted H (the half-width of the channel is located at $x = H$ and the wall at $x = 0$). As the flow is heterogeneous, a non uniform mesh having 200 cells is used. The mesh is refined close to the wall.

At the top of the domain, the PDF entering in the domain, namely for $c_p < 0$, is imposed as

$$\begin{aligned} f(x = H, t; c_p < 0) &= \frac{n_p}{\left(2\pi \langle u'_{f@p} u'_{f@p} \rangle\right)^{1/2}} \\ &\times \exp \left[-\frac{c_p^2}{2 \langle u'_{f@p} u'_{f@p} \rangle} \right]. \end{aligned} \quad (16)$$

At the wall, a full absorption wall condition is imposed meaning that no particle are going back to the flow. This condition reads

$$f(x = 0, t; c_p > 0) = 0. \quad (17)$$

4.2. Fluid flow

In the present study, the fluid flow is imposed through its moments (in terms of mean velocity, mean Reynolds stress, and dissipation). Then in order to avoid of using a model for the prediction of the turbulent flow the profiles that Moser et al. [13] obtained by DNS have been used.

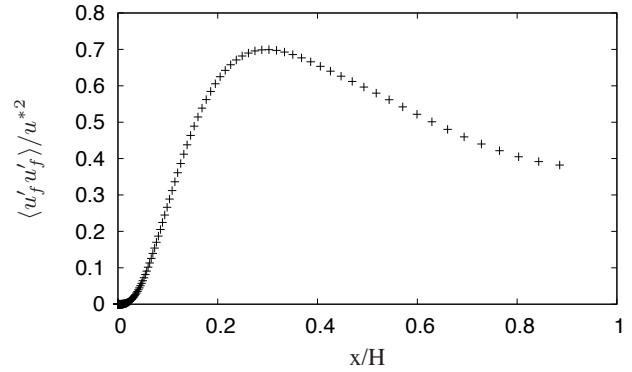


Figure 3: Wall-normal fluid agitation measured by Moser et al. [13] in DNS.

Figure 3 shows the wall-normal Reynolds stress component with respect to the wall distance. As expected in the near wall region $\langle u'_f u'_f \rangle$ decreases quickly up to reach zero at the wall. The Reynolds number

$$Re_{\tau} = \frac{H u^*}{\nu_f} \quad (18)$$

based on frictional velocity, u^* , and the half-width of the channel is 180 and the dimensionless particle diameters $d_{p*} = d_p u^* / \nu_f$ vary between $3 \cdot 10^{-2}$ and 2.9. The Reynolds numbers of the Liu & Agarwal [10] experiment is 309 and 1308 and the dimensionless particle diameters d_{p*} vary between $7 \cdot 10^{-2}$ and 1 for the first Reynolds number and between 0.28 and 4.2 for the second.

The modelling approach has two input parameters: the gas-particle velocity covariance $\langle u'_{f@p} u'_{f@p} \rangle$ and the integral timescale of the fluid turbulence seen by the particles $\tau_{f@p}^t$. The gas-particle covariance is computed by assuming the local equilibrium (Tchen-Hinze theory)[23]. Following this, the gas-particle

covariance is given in terms of the wall-normal Reynolds stress as

$$\langle u'_{f@p} u'_p \rangle = \langle u'_{f@p} u'_{f@p} \rangle \frac{\tau_{f@p}^t}{\tau_{f@p}^t + \tau_p} \quad (19)$$

with $\langle u'_{f@p} u'_{f@p} \rangle \approx \langle u'_f u'_f \rangle$. In a first approximation the fluid integral timescale seen by the particles is assumed to be equal to the one of the fluid $\tau_{f@p}^t \approx \tau_f^t$.

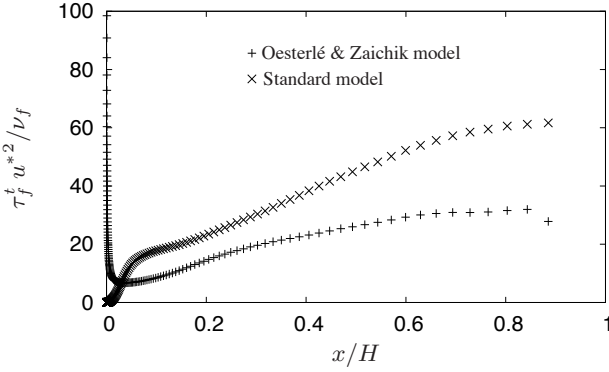


Figure 4: Lagrangian fluid integral time scale predicted by the standard model (+) and by the Oesterlé & Zaichik Model (x) [14].

In the framework of the RANS approach, the Lagrangian fluid integral time scale is commonly computed from the fluid agitation and dissipation as

$$\tau_f^t = \frac{1}{2} \frac{k}{\varepsilon}. \quad (20)$$

Oesterlé & Zaichik [14] proposed to estimate the Lagrangian fluid integral timescale by

$$\tau_f^t = - \frac{\langle u'_f v'_f \rangle}{\langle u'_f u'_f \rangle \frac{\partial V_f}{\partial x}} \quad (21)$$

where the gradient $\partial V_f / \partial x$ is given by the DNS data and the shear stress $\langle u'_f v'_f \rangle$ as well. Figure 4 shows the Lagrangian timescale given by Eq. (20) & (21) with respect to the wall-normal distance. In the near-wall region the standard model predicts that Lagrangian integral timescale tends to zero whereas the "eddy-viscosity" model proposed by Oesterlé & Zaichik [14] predicts that the timescale goes to infinity.

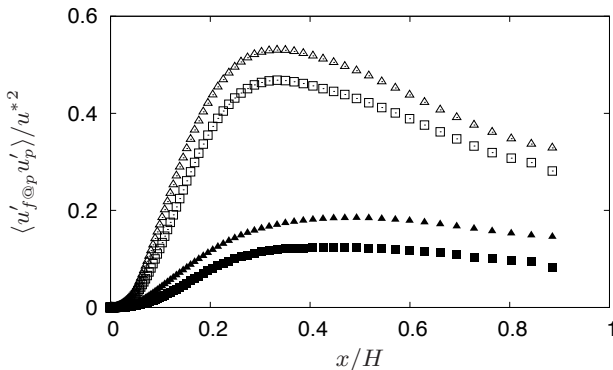


Figure 5: Wall-normal fluid-particle covariance predicted when using the standard model (triangles) and the Oesterlé & Zaichik [14] model (squares). Empty symbols: $\tau_p^* = 10$ and black-filled symbols $\tau_p^* = 100$.

The gas-particle covariance evolution with respect to the wall-normal distance is shown by Figure 5 for two Stokes number $\tau_p^* = 10$ and $\tau_p^* = 100$. As expected the larger the Stokes number is, the smaller the gas-particle covariance is. Figure 5 also shows that the model given by Eq. (21) leads to covariance slightly smaller than the predictions with Eq. (20).

4.3. Physical properties

The Reynolds number is equal to 180. The Stokes number τ_p^* vary between 0.1 and 1000 and the dimensionless particle diameters vary between $2.9 \cdot 10^{-2}$ and 2.9.

4.4. LBM parameters

The numerical simulation have been performed with 20 discrete velocities with 6th order polynomial Hermite expansion ensuring that the five first moments of f_p are accurately computed [6].

5. Particle deposition in vertical channel flow

The deposition rate of particles transported in turbulent vertical channel flow is shown by Figure 6. In LBM simulations, we steady state is reached, the deposition rate is computed by

$$V_d^+ = \frac{1}{u^*} \frac{\int_{-\infty}^0 c_p f_p(x=0) dc_p}{\frac{1}{H} \int_0^H \left[\int_{-\infty}^{+\infty} f_p dc_p \right] dy}. \quad (22)$$

Figure 6 shows that the LBM model predict the inertia-moderated regime, the diffusion-impaction regime and the transition between these two regimes. In diffusion-impaction regime the slope predicted by the LBM is in accordance with slope measured by Liu & Agarwal [10] in their experiments. However, the magnitude of the deposition rate is slightly overestimated by the LBM.

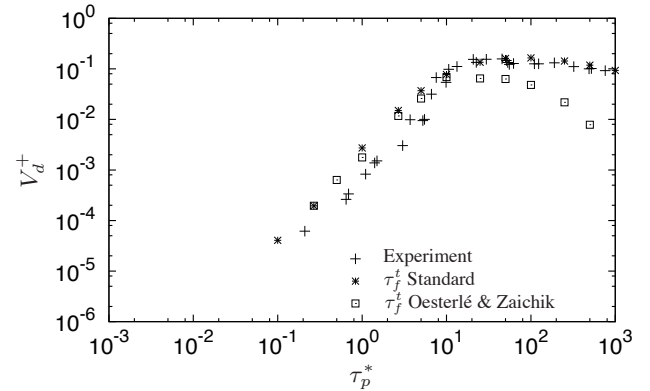


Figure 6: Deposition rate with respect to the Stokes number. Comparison between the experiments of Liu & Agarwal [10], the LBM prediction with τ_f^t predicted by the standard model (20) and by the model proposed by Oesterlé & Zaichik (21) [14].

It is also observed that in the impaction-diffusion regime the standard model for the Lagrangian fluid integral timescale gives the same predictions than the model of Oesterlé & Zaichik [14]. In contrast, some differences are shown by Figure 6 in inertia-moderated regime. Indeed, the "eddy-viscosity" model leads to an underestimation of the deposition whereas the standard model gives predictions in very good accordance with the experiments.

The mean density number of particles with respect to the wall-distance is shown by Figure 7. For small Stokes number ($\tau_p^* = 1$), the profile of n_p is nearly flat from the centre of the

channel to $x/H = 0.2$. When approaching the wall the mean particle density number is increasing and reaches a maximum for $y^+ = 2.5$. Finally from $y^+ = 2.5$ up to $d_p/2$ the particle density is decreasing. For $\tau_p^* = 10$ the trends are the same excepted that in the core of the channel the particle number density is decreasing from the centre to the reach also a peak at $y^+ = 8$. Between $y^+ = 8$ and the wall, n_p is decreasing and reaches a plateau. Finally for $\tau_p^* = 100$, the peak close to the wall vanishes.

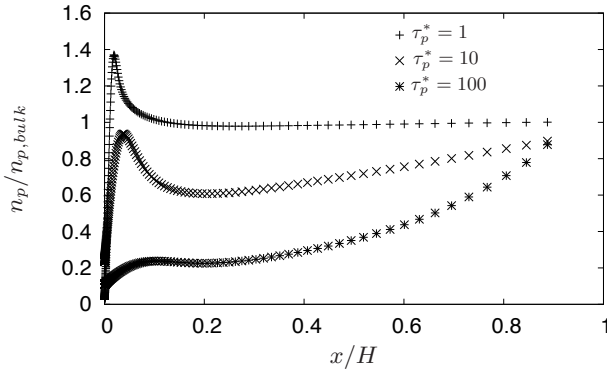


Figure 7: Mean particle number density predicted by LBM for $\tau_p^* = 1, 10, 100$ with respect to the normalized wall-distance.

Figure 8 shows the mean particle velocity with respect to the normalized wall-distance. As expected, when increasing τ_p^* the wall-normal mean particle velocity is increasing.

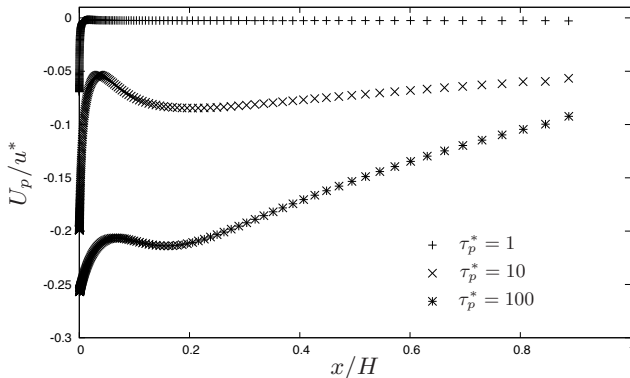


Figure 8: Mean particle velocity predicted by LBM for $\tau_p^* = 1, 10, 100$ with respect to the normalized wall-distance.

The particle velocity covariance is depicted by Figure 9. From the center of the channel towards the wall, the particle kinetic stress is increasing for reaching a peak that is closer to wall for smaller Stokes number. For $\tau_p^* = 100$ and $\tau_p^* = 10$ the variance reaches in a constant positive value very close to the wall. In contrast, for $\tau_p^* = 1$ the particle variance follows the same trend excepted that for $y^+ < 1$ the particle variance becomes negative that is not correct. It is possible that for such a small Stokes number the order of the quadrature has to be increased.

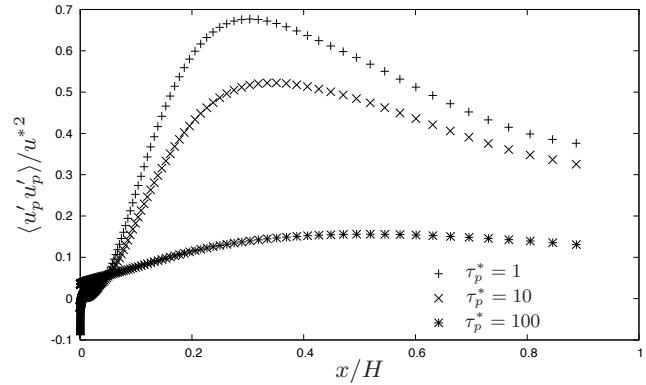


Figure 9: Mean particle variance density predicted by LBM for $\tau_p^* = 1, 10, 100$ with respect to the normalized wall-distance.

6. Conclusion

Lattice Boltzmann Model has been used for solving a kinetic equation describing the interaction of inertial particles with a turbulent flow. The LBM has been applied for predicting the deposition of particles interacting with a turbulent boundary layer. The results show that the deposition rate is in accordance with experimental data for the inertial and impaction-diffusion regime. The transition between inertial and impaction-diffusion regime is well predicted and the slope of the deposition rate is correct. These promising results show that the method seems to be able to predict correctly the gas-particle interaction in the near-wall region but more development are needed. Some trouble stay for the prediction of the moments in the near wall region and some complementary investigations are in progress. The influence of the Reynolds number on the deposition rate predicted by the method is also investigated. Future developments will include different wall interaction such as elastic bounce-back or the addition of the Brownian motion.

7. Acknowledgements

This work was supported by the ANR DEPART project, Grant ANR-12-IS04-0003-01 of the French Agence Nationale de la Recherche and the grant of the Romanian National Authority for Scientific Research CNCS-UEFISCDI, Project Number PN-II-ID-JRP-2011-2-0060.

References

- [1] S. Aguinaga, O. Simonin, J. Borée, and V. Herbert. A simplified particle-turbulence interaction pdf model: application to deposition modelling in turbulent boundary layer. In *Proceedings of the ASME 2009 Fluids Engineering Division Summer Meeting, August 2-6, 2009, Vail, Colorado USA*, pages 2–6, 2009.
- [2] A. S. Berrouk and D. Laurence. Stochastic modelling of aerosol deposition for les of 90 bend turbulent flow. *International Journal of Heat and Fluid Flow*, 29:1010 – 1028, 2008.
- [3] P. L. Bhatnagar, E. P. Gross, and M. Krook. A model for collision process in gases. i.small amplitude processes in charged and neutral one-component systems. *Physical Review*, pages 94–511, 1954.
- [4] I. V. Derevich and L. I. Zaichik. Precipitation of particles from a turbulent flow. *Izvetiya Akademii Nauk SSSR*